Contributions, Geophysical Institute, Kyoto University, No. 11, 1971, 57-70

SOME ASPECTS OF TURBULENT FLUXES NEAR THE GROUND

By

Tatsuo HANAFUSA

(Received September 17, 1971)

Abstract

The observational system including sensors such as the sonic anemometer and new data processing system, HYSAT, has been proved to be used to measure turbulent fluxes and the related atmospheric characteristics.

From the results of preliminary application of this system to the field measurements, the following facts are found.

(i) Concerning the diurnal change of the fluxes, the phase lag of sensible heat flux to the net radiation is small compared with that of momentum flux to the net radiation.

(ii) The thermal balance on the ground surface was certified to contain an error margin of 10%.

(iii) The drag coefficient increases with decreasing wind speed in the wind speed lower than one or two meters per second both over land and over water.

1. Introduction

Knowledge of the vertical turbulent fluxes of momentum, heat and water vapor provides the fundamental information for the study of interaction between larger scale meteorogical phenomena. However, owing to technical limitation in field observation, reliable observational data on the turbulent transport processes in various conditions to be used in the certification of theoretical studies are quite insufficient.

The present author and his collaborators have endeavored to establish a simple and reliable means of turbulent fluxes measurement close to the ground, and completed sonic anemometer-thermometer (Mitsuta [1966], [1968]) and other means of measurements (e.g. Chen & Mitsuta [1967], Sano & Mitsuta [1968], Hanafusa [1970]). However, the labour of data processing and computation prevented extensive measurements of turbulent fluxes, which has been the major difficulty in carrying out extensive study of turbulent flux in various conditions. To save this time loss in data processing and to enable to make on-site and real time analysis of turbulent flux on the field, the present author has proposed and completed the hybrid analog data acquisition system for the atmospheric turbulence called HYSAT.

By the use of the combination of the sensors already developed and the new HYSAT, turbulent fluxes of momentum, heat and water vapor together with related quantities can be obtained on-site in real time and even continuously on the experimental site. A series of experiments on the turbulent fluxes by the present author and his collaborators were possible. In this paper, the preliminary results of the observations performed by the use of HYSAT as the first stage of the extensive study of the turbulent transport processes, are presented.

2. The details of observations

The method of observation is already explained and discussed in other papers (Hanafusa [1971a], [1971b]). A three dimensional sonic anemometer (Mitsuta [1967]) is used for the sensor of the horizontal and vertical components of wind velocity, and a fine wire thermocouple psychrometer (Sano & Mitsuta [1969]) is used for the sensor of the dry- and wet-bulb temperatures. The on-site data processing of the outputs of these sensors is made by the hybrid analog data acquisition system developed by the author (Hanafusa [1971b]) with the procedure proposed also by the author (Hanafusa [1971a]).

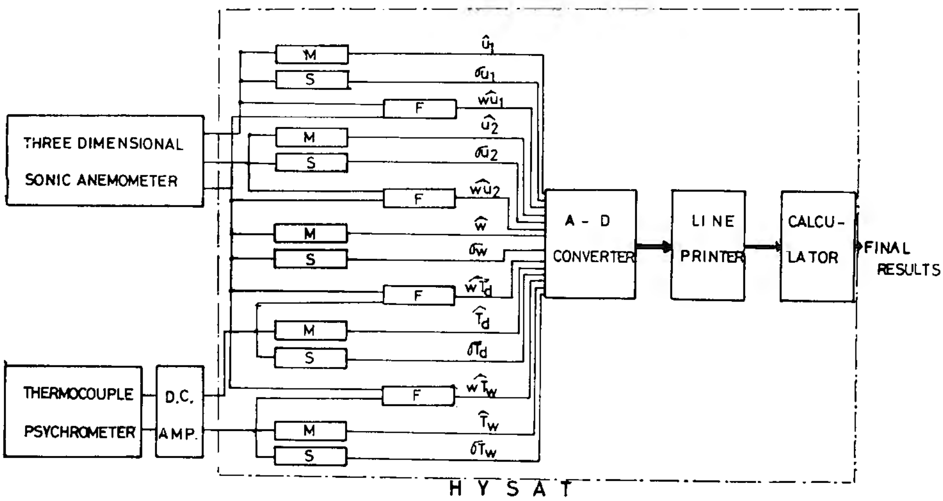

M : Mean-meter, S : Sigma-meter, F : Flux-meter

Fig. 1. The block diagram of the observational system.

The outputs of the sonic anemometer are supplied directly and those of the fine wire thermocouple psychrometer are amplified by 2000 to 5000 times and then supplied to the HYSAT. The mean values and the standard deviations of the horizontal and vertical components of wind velocity, the dry- and wet-bulb temperatures and the covariance of each component with the vertical velocity component are processed by HYSAT. The sampling rate of digital part was once a minute. The cold point of the thermocouple of psychrometer was placed in the water of thermos whose temperature was remotely measured by a thermister thermometer once or twice an hour. The block diagram of the observation is shown in Fig. 1.

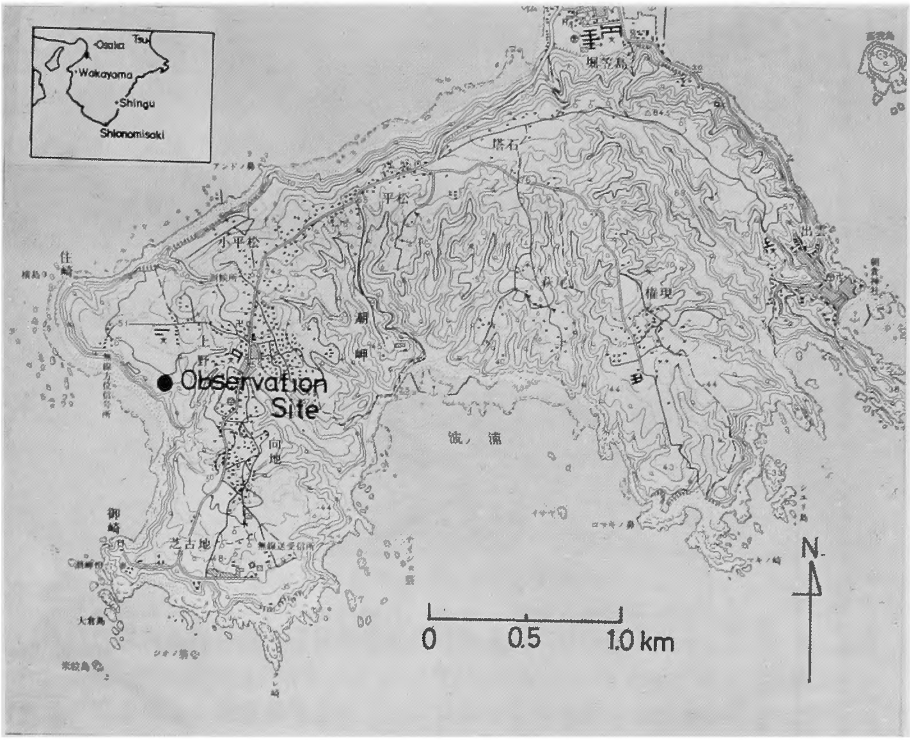

Fig. 2. Map of the observation site.

Shionomisaki– The first experiment was made on the testing site of the Shionomisaki Wind Effects Laboratory of Kyoto University, which is located at the southern end of Honshu Island, as shown in Fig. 2. The surface area of the testing site is bare soil of about 50 m in diameter in the open flat farm land. The sensors were installed at the height of 1.5 m. Besides the sensor for turbulent flux measurement, the net radiation sensor (supplied by Beckman & Whitley Inc.) was installed at the height of 1.0 m and mean profile sensors of wind, air temperature and humidity were installed on the tower of 5.0 m and those of soil temperature sensors under the ground.

The observation was made from 19 to 21 of August 1969. The results are summarized in Table 1. The mean values of wind speed, air temperature and humidity, shown in this table, are the values at the height of 1.5 m obtained by the mean-meters. The mean wind speed is vector mean wind speed and is reliable enough down to a few centimeters per second as the sonic anemometer is sensible down to very low wind speed (Mitsuta, Miyake, & Kobori [1967]). The rest of the parameters shown in this

Table 1. Vertical turbulent fluxes and related parameteters over bare soil.

Notations used in Tables 1–3 are as follows; U: mean wind speed, T_d: mean air temperature, $\bar{q}$: mean specific humidity, τ: momentum flux, H: sensible heat flux, L: latent heat flux, σw: variance of vertical wind velocity, σt: variance of air temperature, u_*: friction velocity, C_d: drag coefficient

Run No.	Date	Time	Cloud Cover	Cloud Form	U (cm/s)	T_d (°C)	$\bar{q}$ ($\times 10^{-3}$ g/g)	τ (dyne/cm²)	H (mW/cm²)	L (mW/cm²)	σw (cm/s)	σt (°C)	u* (cm/s)	C_d ($\times 10^{-2}$)
3	69/8/19	09:01–09:55	2	Cu	182	27.2	18.3	0.50	5.63	38.77	44	0.57	20	1.26
4–1	〃	09:58–10:42	3	Cu	201	27.2	18.2	0.07	8.40	12.73	52	0.58	8	0.15
4–2	〃	10:43–11:34	3	Cu	151	28.1	18.6	0.65	11.34	14.07	48	0.81	23	2.37
5	〃	11:36–12:30	2	Cu	143	27.9	18.5	0.36	12.39	16.25	39	0.99	17	1.46
6	〃	13:00–13:55	1	Cu	99	27.9	17.4	0.67	14.83	16.67	47	0.94	24	5.70
7	〃	14:30–15:22	1	Cu	102	27.2	19.6	0.05	11.34	17.26	32	0.76	6	0.38
9	〃	17:19–18:30	1	Cu	146	26.5	19.1	0.07	1.05	21.88	24	0.48	8	0.27
10	〃	18:33–19:39	2	Cu	142	25.8	18.4	0.03	8.53	—	21	0.27	5	0.12
11	69/8/20	10:37–11:59	4	Cu	66	29.1	19.6	0.28	13.19	18.77	33	0.87	15	5.30
12	〃	12:00–12:59	1	Cu	70	29.2	19.6	0.15	14.74	14.28	42	0.80	11	2.51
13	〃	13:34–14:10	2	Cu	242	28.6	19.5	0.75	8.48	19.78	53	0.54	25	1.06
14	〃	14:17–15:04	3	Cu, As	313	28.1	18.7	0.62	6.76	30.62	54	0.43	23	0.53
15	〃	15:58–16:56	4	Cu, As	257	27.5	18.8	2.39	3.61	28.39	48	0.45	46	3.01
16	〃	17:07–18:10	6	Ac	362	26.8	18.5	1.14	1.22	29.99	68	0.21	31	0.72
17	〃	18:11–19:06	5	Ac, As	204	26.2	18.1	0.27	0.21	32.17	36	0.13	15	0.55
18	〃	19:23–20:21	3	Ac	107	25.5	17.2	0.10	1.43	—	16	0.13	9	0.71
19	〃	20:26–21:23	–	—	165	25.9	17.6	0.45	−0.08	12.85	25	0.13	19	1.37
20	〃	22:43–23:38	–	—	17	24.9	18.3	0.06	1.26	10.58	2	0.24	7	16.26
21	69/8/21	01:49–02:33	–	—	67	24.1	17.9	0.02	1.09	11.21	6	0.24	4	0.38
22	〃	04:43–05:34	5	Ns	70	24.5	18.3	0.02	−0.04	4.07	11	0.25	4	0.31
23	〃	05:43–06:27	7	As, Ac, Cu	30	25.0	18.3	0.09	0.42	8.11	5	0.32	8	7.89
24–1	〃	06:49–07:33	7	As, Ac, Cu	56	26.7	19.3	0.06	1.09	8.48	12	0.30	7	1.53
24–2	〃	07:49–08:33	7	As, Ac, Cu	53	26.8	19.1	0.13	0.38	9.37	14	0.23	11	3.95
24–3	〃	08:34–09:27	7	As, Ac, Cu	59	27.9	17.9	0.06	3.70	4.75	18	0.72	7	1.41
25	〃	12:36–13:33	9	As, St, Cu	184	27.0	16.3	0.21	7.35	15.04	34	0.59	13	0.51
26	〃	13:48–14:32	9	Cu, Ac, St	164	28.2	16.1	0.21	10.71	33.73	29	0.86	13	0.66
27	〃	15:05–16:02	4	Cu, Ci	178	28.3	18.2	0.20	5.75	28.14	33	0.56	13	0.53
28	〃	16:03–17:00	8	Cu, Ci	207	27.1	18.4	1.02	2.90	28.14	35	0.42	29	1.98
29	〃	17:12–18:09	9	Cu, As	98	26.7	18.7	0.11	1.30	26.71	29	0.27	10	0.96

table is also obtained by HYSAT. In this table the latent heat flux is shown instead of water vapor flux.

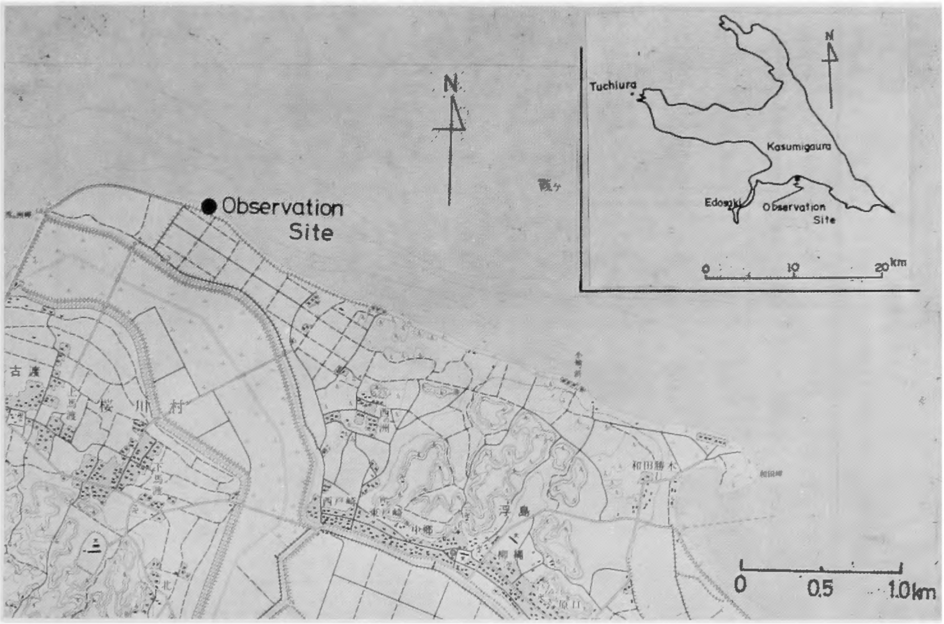

Fig. 3. Map of the observation site.

Kasumigaura– The turbulent flux measurement over water on the Lake Kasumigaura, the second largest lake in Japan near Tokyo, has been made as a part of a project for the study of evaporation (See Fig. 3). The first experiment was made in December 1969, the results of which are already published as a part of the report of the project (Mitsuta, Hanafusa, Maitani & Fujitani [1970]). The main part is reproduced in Table 2. The second experiment was made in the same season of the next year and the results are shown in Table 3. In this case the observation was made on the tower of 1.5 m from the water surface standing about 10 m from the shore. The mean profile and other relating quantities are measured by the other groups participating the project and will be reported in the separate paper. The results shown in these tables are only in the case where wind blows from water to land.

3. Discussions

Diurnal changes of turbulent fluxes– As the almost continuous measurement of turbulent flux under stationary weather condition was made on Aug. 20, 1969 at Shionomisaki as shown in Table 1, the time changes of turbulent fluxes of momentum, sensible and latent heat sampled over about one hour are shown in Fig. 4 together with time changes of the net radiation, soil temperature, wind speed, air temperature

Table 2. Vertical turbulent fluxes and related parameters over water (Mitsuta et al. [1970])

Run No.	Date	Time	U (cm/s) [m/s]*	T_d (°C)	τ (dyne/cm^2)	H (mW/cm^2)	L (mW/cm^2)	σ_w (cm/s)	u* (cm/s)	C_d ($\times 10^{-3}$)
69–K– 3	69/12/11	21:01–21:37	536 [4.3]	6.6	1.32	0.4	6.1	17	33	5.90
K– 4	〃	22:27–23:21	622 [5.1]	6.4	0.67	−0.6	9.7	19	23	2.05
K– 5	69/12/12	00:33–01:27	566 [—]	6.9	0.57	−2.4	2.9	22	21	1.62
K– 6	〃	02:36–03:30	279 [2.3]	6.5	0.18	−0.8	−1.9	20	12	—
K– 7	69/12/13	10:56–11:21	536 [1.4]	7.7	0.89	5.0	0.7	24	27	5.17
K– 8	〃	11:36–12:29	1020 [7.7]	9.1	1.51	−2.8	1.3	56	35	2.04
K– 9	〃	14:04–14:27	1178 [8.8]	9.2	1.01	3.0	−7.9	57	29	1.05
K–10	〃	16:04–16:48	827 [6.4]	6.6	1.88	3.7	−6.9	—	39	3.68
K–11	〃	21:38–22:07	(570) [—]	3.0	—	1.0	7.7	—	—	—
K–12	69/12/14	00:43–01:23	284 [2.3]	—	0.45	−0.1	4.1	—	19	6.87
K–13	〃	06:37–07:10	325 [3.1]	1.6	0.59	2.4	4.0	—	22	4.91
K–14	〃	09:22–10:15	232 [2.2]	4.1	0.43	2.8	3.6	24	18	7.06

* Mean wind speed was measured by the small cup anemometer at 1.5 m height.

Table 3. Vertical turbulent fluxes and related parameters over water

Run No.	Date	Time	$\bar{U}$ (cm/s)	$\bar{T}_d$ (°C)	τ (dyne/cm^2)	H (mW/cm^2)	L (mW/cm^2)	σw (cm/s)	u* (cm/s)	σt (°C)	C_d $\times 10^{-3}$
70–K– 1	70/11/17	14:40–15:10	297	10.3	0.32	4.96	—	13	16	0.19	3.03
K– 2	〃	15:40–16:10	209	11.4	0.28	−1.89	3.74	12	15	0.11	5.33
K– 3	〃	24:00–01:00	195	9.0	0.22	−0.62	0.29	10	14	0.29	4.89
K– 4	70/11/18	01:00–02:00	270	8.8	0.05	0.10	2.27	12	7	0.14	0.60
K– 5	〃	02:00–03:00	207	8.8	0.18	−1.20	2.73	10	12	0.13	3.48
K– 6	〃	03:00–04:00	151	8.3	0.18	−0.24	1.34	12	12	0.15	6.67
K– 7	〃	04:00–05:00	222	8.6	0.24	−0.74	0.42	10	14	0.18	4.14
K– 8	〃	05:00–06:00	208	8.6	0.10	−0.52	1.93	10	9	0.10	1.85
K– 9	〃	06:00–06:30	160	8.5	0.20	−0.63	3.19	9	13	0.43	6.64
K–10	〃	08:10–09:00	197	9.2	0.17	−0.62	—	9	12	0.14	3.76
K–11	〃	09:00–10:00	84	10.2	0.13	−2.76	—	8	11	0.38	15.73
K–12	〃	10:00–11:00	144	10.6	0.23	−0.65	—	7	14	0.28	9.16
K–13	〃	11:00–12:00	138	11.8	0.12	−1.45	—	6	10	0.16	5.30
K–14	〃	12:00–13:00	276	12.4	0.39	−1.30	—	11	18	0.08	4.27
K–15	〃	13:00–14:00	133	12.9	0.20	−1.65	—	5	13	0.25	9.38
K–16	〃	14:00–15:00	85	13.1	0.15	−2.17	—	4	11	0.25	17.16
K–17	〃	15:00–16:00	93	12.8	0.06	−2.03	—	6	7	0.24	5.43
K–18	〃	16:00–16:30	88	12.6	0.33	−2.27	—	5	17	0.10	35.77

and specific humidity. The turbulent fluxes also show distinct diurnal changes as well as other meteorological parameters. To compare the diurnal changes of flux with those of other parameters, harmonic analysis of these quantities from 1000 JST of 20th to 1000 of the next day were made and shown in Table 4. In the analysis, the values of turbulent fluxes are smoothed to have the estimated values at equal length time intervals. In this table, results of the same kind of study made at the same place in 1967, which are analyzed in digital method (Mitsuta, Hanafusa & Maitani [1970]), are also shown for comparison.

Table 4. Results of harmonic analysis of physical quantities

$$X=\bar{X}+A\sin(\theta t+\phi_1)+B\sin(2\theta t+\phi_2)+\ldots\ldots$$

t=0 at midnight, J.S.T.

1969's observation

	$\bar{X}$	A	B	ϕ_1 (degree)
N.R. (mW/cm^2)	16.8	34.5	19.2	−95 (12:20)*
H (mW/cm^2)	3.4	4.4	3.2	−102 (13:00)
L (mW/cm^2)	15.5	10.0	3.7	−161 (16:40)
τ ($dyne/cm^2$)	0.39	0.55	0.36	−146 (15:40)
$\bar{U}$ (m/s)	1.12	1.06	0.64	−154 (16:20)
$T_{1.5m}$ (°C)	26.4	2.4	0.7	−105 (13:00)
T_{-5cm} (°C)	28.7	2.6	0.9	−137 (15:00)

* The time when $\theta t+\phi_1=90°$

1967's observation (Mitsuta et al. [1970])

	$\bar{X}$	A	B	ϕ_1 (degree)
N.R. (mW/cm^2)	19.8	38.8	17.9	−89 (12:00)*
H (mW/cm^2)	1.17	2.03	0.10	−91 (12:00)
L (mW/cm^2)	5.34	7.56	1.51	−111 (13:20)
τ ($dyne/cm^2$)	0.73	0.41	0.15	−152 (16:00)
$\bar{U}$ (m/s)	2.10	0.88	0.35	−195 (19:00)
$d\theta/dz$ (°C/cm)	8.0	19.9	6.5	−99 (12:40)
$T_{0.4m}$ (°C)	28.5	2.7	0.4	−112 (13:20)
$T_{0.6m}$ (°C)	27.2	1.7	0.5	−120 (14:00)

Both days are clear summer days, but the heat fluxes in the present case are twice as large as in the case in 1967. The phases of the diurnal components of the net radiation, N.R. and sensible heat flux, H, are almost the same for both cases and the maxima around the noon. This shows that the surface temperature is directly determined by the net radiation as seen in Fig. 4 and the sensible heat flux also follows immediately the surface temperature. The maxima of the momentum flux are also nearly the same for both case, but they are delayed about 3 or 4 hours from the net radiation and the sensible heat flux. This delay time shows the response time of planetary boundary layer motion to the change of energy supply from the bottom. Condensation of water vapor in the planetary boundary layer was not seen in both cases.

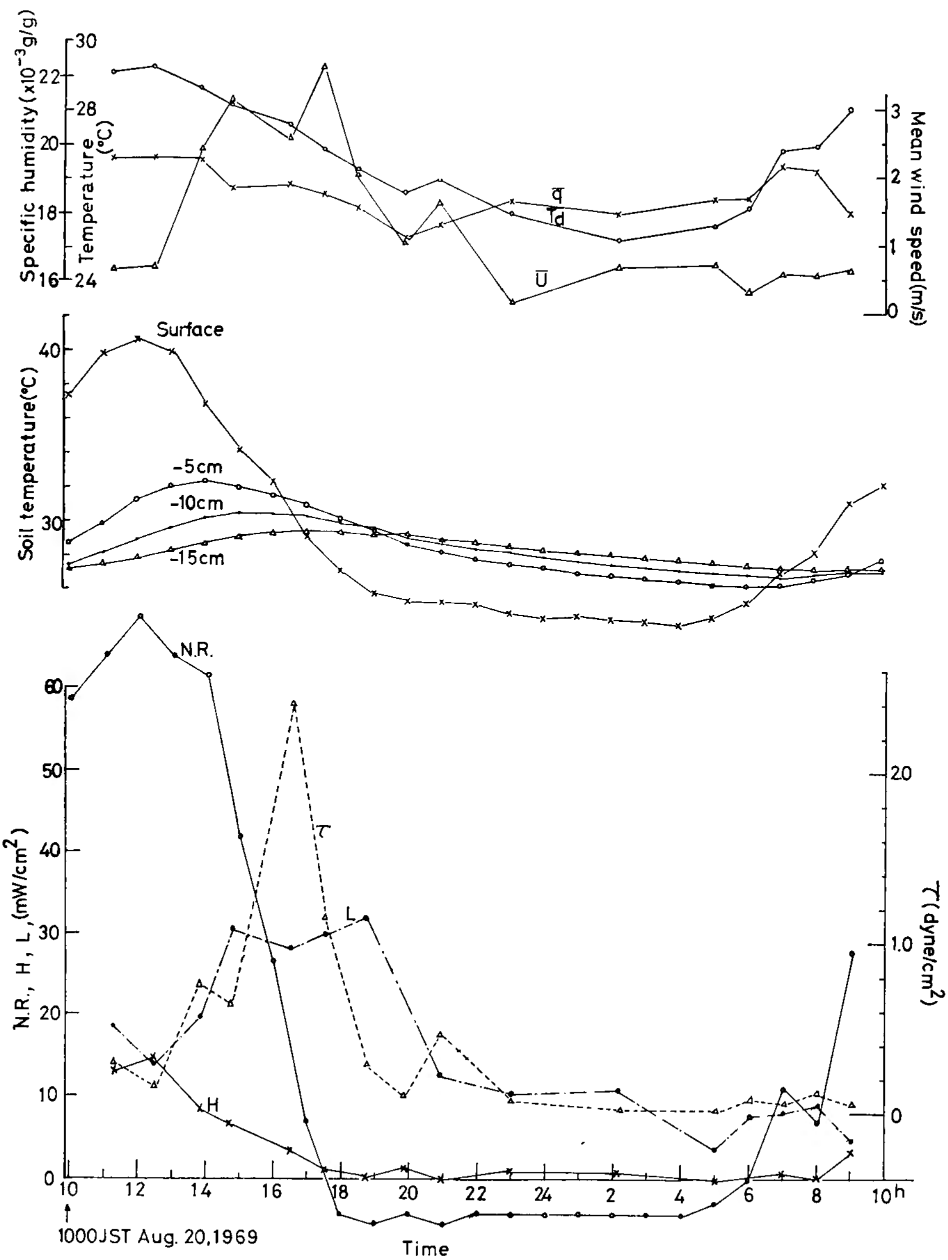

Fig. 4. An example of the time variations of vertical fluxes and mean quantities.

The evaporation from the surface shows a quite different peak occurrence. The maximum of the present case (1970) is at 16:40 while that of the previous case (1967) is at 13:20. The reason for the large difference is not clear but it may result from the difference of conditions of soil moisture near the surface. In the previous observation (1967), the surface layer of the ground was dried up during the sunny days before the experiment. While in the present experiment (1970) the surface was wet from rain fall of 6mm in the early morning of the day on which the observation was interrupted. Therefore, in the latter case, the surface condition was nearly wet. However, a quantitative measurement of moisture in the ground soil was not made and further dicussion is difficult at present.

Thermal balance– As the soil temperature profile and the net radiation were measured together with the turbulent fluxes, the thermal balance on the ground surface can be checked entirely from the observed data of the present observation without any assumptions. The total incoming flux of radiative energy on the ground surface can be approximated by the integrated value of the net radiation at 1 m from the ground. Then, the total incoming radiative energy in the time period from 1000 JST of Aug. 20 to 1000 JST of the next day shown is estimated to be 341 ly/day by graphical integration. The sensible and latent heat losses from the ground surface are also approximated by the turbulent fluxes of sensible and latent heat at the height of 1.5 m, the total values of which are 72 and 325 ly/day respectively by graphical integration. Therefore, the difference of the incoming radiation and outgoing fluxes becomes 55 ly/day heat loss from the ground surface, which must be compensated from the ground. The outgoing flux, B, from the ground across the surface over the time interval of T, is shown as follows.

$$B = c\rho \int_0^T \int_0^d \frac{\partial \theta}{\partial t} dzdt + \lambda \int_0^T \left.\frac{\partial \theta}{\partial z}\right|_d dt \qquad (1)$$

where $c\rho$ is volume specific heat of the soil, θ, soil temperature, λ, heat conductivity of the soil and z, the depth, d, being the reference depth. The total value of B of this day was computed from the soil temperatures shown in Fig. 4 and to be 12 ly/day heat loss from the soil surface. The values of parameters of $c\rho$ and λ used in this computation were also observed values in the test field at the same time and were 0.632 cal cm^{-3} deg^{-1} and 1.74×10^{-3} J./cm.s.degs. respectively. This heat loss is reasonable in the sense that the amount is not enough large to balance the aerial heat loss shown above. The residue is 43 ly/day. The reason for the residue is not clear. However, we can say that the radiative energy input to the ground is compensated by the sensible and latent heat fluxes and heat from the ground within errors of 10% during this day.

Time change of flux– The averaging time of data for turbulent flux estimation is determined to the low frequency limit of the frequency range which does not contribute to transport processes. And the frequency chosen in the present system, HYSAT of 10 cps (Hanafusa [1971a]) is high enough in the boundary layer not to lose any contributions of high frequency fluctuations of physical entities to the flux. The sampling duration must be long enough not to lose contributions of low frequency fluctuations to the flux. According to the results obtained by Businger et al.

[1967], the cospectra between vertical velocity and temperature show relatively high value down to 0.003 cps or so. This means that the sampling duration should be long enough compared to this frequency. Therefore, the sampling duration of about a half to one hour was chosen in the present experiments.

However, Fig. 4 shows that there are time intervals in which appreciable time changes of fluxes within an hour is expected. In order to study the time change rate of turbulent flux, the shorter sampling duration must be used. Fig. 5 and 6 show the time change of the sensible heat flux during short time periods in the observation shown in Fig. 4.

Fig. 5 represents an example for the time period in which time change of heat flux is relatively small. While Fig. 6 represents the case in which time change of flux is relatively large. These curves shown in both figures represent the time changes of turbulent heat fluxes with sampling duration of 5, 10 and 15 min. The time change curves of heat flux for 5 min. sampling duration show rather large fluctuations from time to time. The reason for fluctuations in time series of heat flux for 5 min. sampling duration is not clear, though their smoothed curves correspond fairly well to heat

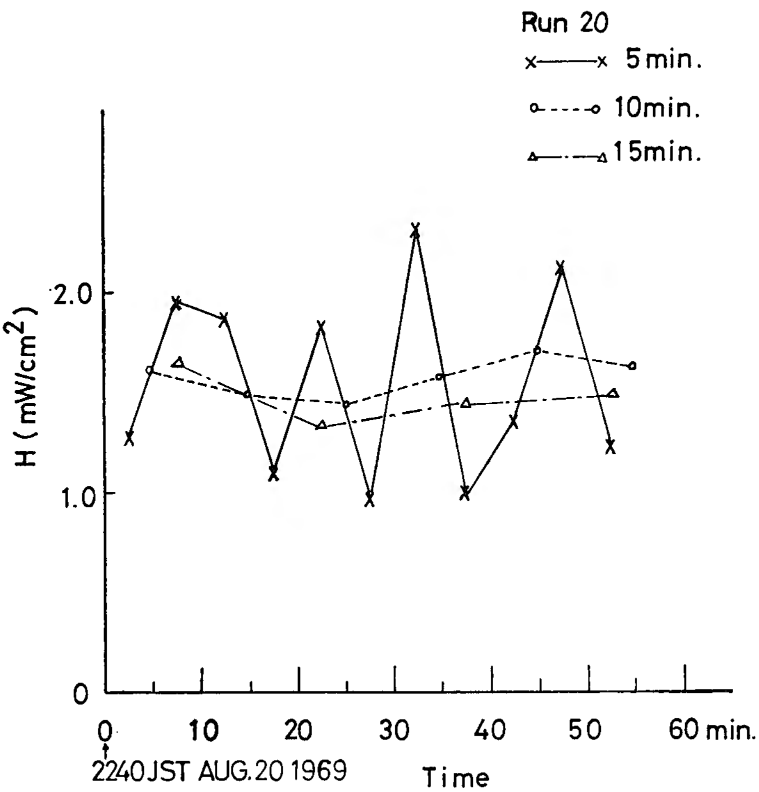

Fig. 5. An example of the time changes of the sensible heat flux during short time periods in Run No. 20.

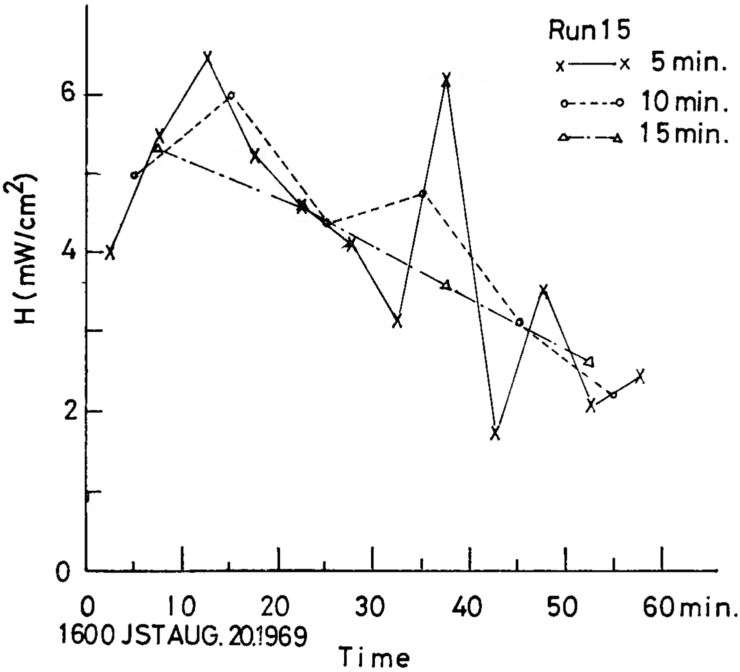

Fig. 6. An example of the time changes of the sensible heat flux during short time periods in Run No. 15.

fluxes over 10 min. or 15 min. sampling duration. It may be said that it should be recommended to make the sampling duration longer than 10 min. in order to study the time change of turbulent flux. Furthermore, to make a detailed study of the time change of the flux, it must be correlated with the time change of the profile of that entity.

Drag coefficient– The drag coefficients computed from the drag force represented by the momentum flux and mean wind speed obtained by the sonic anemometer during the whole observations [except '69 Kasumigaura] are plotted for wind speed in Fig. 7. In the case of '69 Kasumigaura observation the mean wind speed shown in this figure is the value at 1.5 m height measured by the small cup anemometer which was used in computing drag coefficient and is shown as the brackets in Table 2. The drag coefficient obtained over the Lake Kasumigaura is a little larger than the value expected over open water, which may indicate that modification of airflow begins even on the water near the shore. As is clearly seen, the values of the drag coefficient is not independent of wind speed but increases with decreasing wind speed in light wind lower than a few meter/sec or so. This region has never been subjected to experiment in the atmosphere, because the error of wind speed measurement in low wind speed region was difficult owing to the threshhold of the anemometer. From the theoretical point of view, increasing of the drag coefficient in low wind speed region is not unreasonable, because the flow tends to be laminar in low wind speed

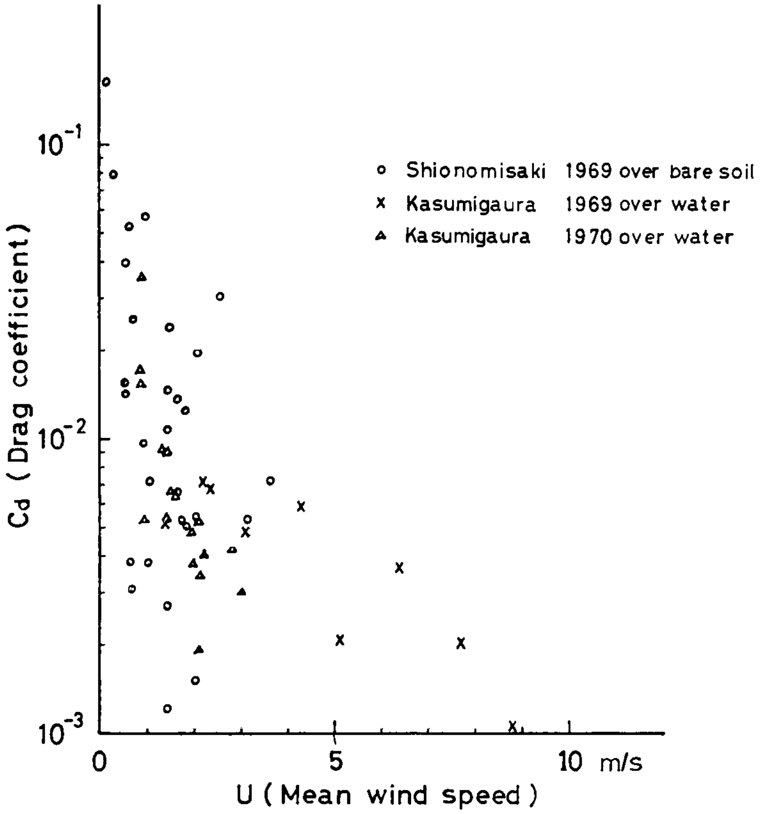

Fig. 7. Dependence of the drag coefficient C_d on the mean wind speed at 1.5 m.

region, especially over water (Hill [1962]).

The present results show that this is also true even over land surface. This point must be studied in datail together with the effect of thermal stability of air current.

4. Conclusion

The results shown in this paper demonstrate that the observational system including the sonic anemometer, other sensors and a new data processing system HYSAT can be used to measure turbulent fluxes and the related atmospheric characteristics. By this system, the measurement can be done on-site and in real time, and the turn arround time of the experiment has been greatly shortened.

From the results of preliminary application of the system shown in this paper, the diurnal changes of turbulent fluxes are analyzed and it is proved that the phase lag of sensible heat to the net radiation is small but that of momentum flux to the net radiation is rather large. The thermal balance on the ground surface was certified to have an error marging within 10% only from the observed quantities of every term of the heat balance equation. It is also found that the drag coefficient increases with decreasing wind speed in wind speed less than one or two meters per second both over land and over water.

Acknowledgements

The present author wishes to express his sincere thanks to Professor R. Yamamoto of Meteorological Research Institute, and Associate Professor Y. Mitsuta of Disaster Prevention Research Institute, Kyoto University for their encouragements and discussions throughout the present study, and also to Messrs. T. Maitani and T. Fujitani for their appreciated cooperations in these observations.

References

Businger, J. A., M. Miyake, A. J. Dyer and E. F. Bradley, 1967: On the direct determination of the turbulent heat flux near the ground. J. Appl. Met., **6**, 1025–1032.

Chen, H. S. and Y. Mitsuta, 1967: An infrared absorption hygrometer and its application to the study of the water vapor flux near the ground. Special Contributions of Geophysical Inst., Kyoto Univ., **7**, 83–94.

Hanafusa, T., 1970: A simple method for the measurement of water vapor flux. J. Met. Soc. Japan, Ser. II, **48**, 259–262.

Hanafusa, T., 1971a: A new method of on-site data analysis of turbulent transports near the ground. Contributions of Geophysical Inst., Kyoto Univ., **11**, 35–46.

Hanafusa, T., 1971b: New hybrid analog data acquisition system for atmospheric turbulence (HYSAT). Contributions of Geophysical Inst., Kyoto Univ., **11** 47–56.

Hill, M. N., 1962: *The sea,* Interscience Publishers, New York,

Mitsuta, Y., 1966: Sonic anemometer-thermometer for general use. J. Met. Soc. Japan, Ser. II, **44**, 12–24.

Mitsuta, Y., M. Miyake and Y. Kobori, 1967: Three dimensional sonic anemometer-thermometer for atmospheric turbulence measurement. WDD Technical Note, Disaster Prevention Res. Inst., Kyoto Univ. Occasional Report, 37–56.

Mitsuta. Y., 1968: Application of sonic anemometer-thermometer to the studies of vertical eddy transport processes in the atmospheric boundary layer. Special Contributions of Geophysical Inst., Kyoto Univ., **8**, 45–60.

Mitsuta, Y., T. Hanafusa and T. Maitani, 1970: Experimental studies of turbulent transfer processes in the boundary layer over bare soil. Bull. Dis. Prev. Res. Inst., Kyoto Univ., **19**, 4, 45–58.

Mitsuta, Y., T. Hanafusa and T. Fujitani, 1970: Measurement of eddy momentum flux near the ground. Special Contributions of Geophysical Inst., Kyoto Univ., **10**, 85–91.

Sano, Y. and Y. Mitsuta, 1968: On the dynamic response of the hygrometer using fine thermocouple psychrometer. Special Contributions of Geophysical Inst., Kyoto Univ., **9**, 61–70.